Green synthesis and characterization of silver nanoparticles from *Tagetes erecta* flowers

RAMAZAN ERENLER[a,*] CENGIZ TEMIZ[b], ILYAS YILDIZ[a], YUSUF YANAR[c], CIGDEM OZYIGIT[c]
[a]*Department of Chemistry, Faculty of Arts and Sciences, Tokat Gaziosmanpasa University, 60250 Tokat, Turkey*
[b]*Department of Electronic and Automation, Alapli Vocational High School, Zonguldak Bulent Ecevit University, 67850 Zonguldak, Turkey*
[c]*Department of Plant Protection, Faculty of Agriculture, Tokat Gaziosmanpaşa University, 60250 Tokat, Turkey*

Nanotechnology is emerging as a rapidly growing field with its application in Science and Technology to produce new materials. In this study, silver nanoparticles were synthesized using an aqueous extract of *Tagetes erecta* L. flowers. The development of silver nanoparticles (AgNPs) was identified by spectral (UV-Vis absorption, FTIR, EDX, and XRD), and microscopic (SEM) analyses. The formation of AgNPs was confirmed by the appearance of the absorption peak at 422 nm. In addition, SEM analysis displayed the spherical-shaped nanoparticles. The crystalline nature of AgNPs was revealed by XRD analysis with an average size of 80.10 nm.

(Received January 24, 2021; accepted October 7, 2021)

Keywords: Tagetes erecta L., Silver nanoparticles, Spectroscopy, Green chemistry

1. Introduction

Aromatic and medicinal plants play an important role in drug discovery and development due to the bioactive compounds they contain [1-6].

Nanoparticles (NPs) are considered the basic building blocks of nanotechnology. The range of nanotechnology is the most dynamic research area in materials science, and the synthesis of nanoparticles (NPs) is increasing significantly worldwide. NPs show completely new or improved properties, taking into account certain properties such as size (1-100 nm), shape, and structure. There is an increasing demand for noble metal (Au and Ag) NPs as they have various applications. Silver nanoparticles (AgNPs) have a significant specific surface area that results in considerable biochemical reactivity, catalytic activity, and atomic behavior compared to larger particles of the same chemical composition. AgNPs received a significant interest due to a large variety of applications such as biomedicine, information storage, energy generation, catalysis, biological sensors, optoelectronics, DNA sequencing, biological activity [7-10]. The silver nitrate solution and a natural reducing agent are key requirements for the green synthesis of AgNPs. The biomolecules such as vitamins, polysaccharides, alkaloids, amino acids, proteins, saponins, terpenes, phenolics are used for silver ion reduction and stabilization to synthesize the silver nanoparticles. [11]. The synthesis of AgNPs has become an important research area due to their diverse applications in industrial, pharmacological, and medical fields as they exhibit good antifungal, anti-inflammatory, anticoagulant, antibacterial, antioxidant, antiviral, thrombolytic, cytotoxic, and photocatalytic properties [12, 13].

AgNPs were synthesized from *Taxus baccata* extract that revealed the considerable anticancer activity on MCF-7 cells [14]. In addition, it was reported that AgNPs synthesized from *Helicteres isora* stem bark extract displayed significant antimicrobial, antioxidant, and anticancer activity [15].

Traditional methods for producing NPs are expensive, toxic, and non-environmentally friendly. Hence, naturally occurring sources have been employed for the synthesis of nanoparticles to overcome these problems [16, 17]. Green synthesis can be classified as usage of a) microorganisms such as fungi, yeasts, bacteria, and prokaryotes, b) plants, c) templates such as membranes (thylakoid membranes, lymphocyte cell membranes), DNA, viruses and diatoms [18, 19] to obtain metal nanoparticles. The plant-based synthesis of nanoparticles is considered the best method [20].

The genus *Tagetes* has 122 species belonging to the Asteraceae family. *Tagetes erecta* Linn., an ornamental flower, is commonly known as Marigold [21]. *T. erecta* has been used in folk medicine to treat various illnesses such as colds, bronchitis, and rheumatism. In addition, it is known that the juice obtained from flowers and leaves has aphrodisiac, diaphoretic, emetic, antipyretic, muscle relaxant, liver tonic, edema reliever, and healer of menstrual irregularity properties [22]. Phytochemical investigation on *T. erecta* flowers revealed the presence of carotenoids such as lutein, and zeaxanthin [23]. Lutein palmitate is found in *T erecta* flowers as a major pigment [24]. Lutein, the chief carotenoid found in *T. erecta* flowers was reported to have a protective effect against some illnesses such as muscular diseases, cardiovascular diseases, cancer, oxidative damages. Furthermore, the extracts of *T. erecta* flowers revealed antimicrobial, antimutagenic, antiviral, anti-inflammatory, antitumor,

anti-immunostimulating, insecticidal, nematocidal, and analgesic activities [25].

In the previously reported work, *T. erecta* flowers extract was obtained by boiled distilled water for the synthesis of silver nanoparticles. Hexane and acetone, toxic chemicals were used for extraction as well. The extraction with boiled water can lead to the decomposition of some secondary metabolites. So, the extraction protocol of our study was completely different from the reported study [26]. Hence, the secondary metabolites in the extract that reduced silver ions were completely different in our study compared to the previous study.

In this study, nanoparticles were synthesized from *T. erecta* flowers, and spectroscopic methods such as UV-Vis, FTIR, XRD, and EDX were used to identify the green synthesized silver nanoparticles; the morphology was evaluated by SEM analysis. The secondary metabolites in the *T. erecta* flowers are responsible for the reduction of silver ions.

2. Experimental

2.1. Plant material

Tagetes erecta L. flowers were collected from the Aromatic and Medicinal Plant Field of Tokat Gaziosmanpasa University (Turkey) during the harvesting stage in 2020.

2.2. Synthesis of silver nanoparticles

Tagetes erecta (50 g) was powdered and heated in distilled water (200 mL) at 80ºC for 3 hours. After filtration, this mixture was reacted with $AgNO_3$ solution (36.8 mM, 200 mL) at 70ºC for 2 hours while connecting the condenser to the reaction flask. The colour change from yellow to dark brown revealed the formation of silver nanoparticles. After centrifugation at 15000 rpm for 30 minutes, the formed silver nanoparticles were washed with distilled water. Then, the AgNPs were dried thoroughly by lyophilization [27].

2.3. X-ray diffraction (XRD) analysis

The structure of AgNPs was evaluated by X-ray diffraction (XRD) analysis. Empyrean, Malvern Panalytical diffractometer was used to record the XRD pattern. The operation voltage was fixed as 45 kV at a 40 mA with Co-kα1 radiation (λ = 1.54 Å). The diffracted intensity was recorded in the region of 2θ from 20º to 90º at 0.02º/min. The particle size was assessed by Dynamic Light Scattering (DLS) on a DelsaNano C instrument.

2.4. Scanning Electron Microscopy (SEM) Analysis

SEM analysis revealed the nanoparticles morphology. The particles were powdered in an agate mortar to make the uniform distribution. Later, the nanoparticles were spread on strap with carbon band and gold plated under vacuum. SE (Secondary electron) mode with high vacuum was applied for analysis. The elemental analysis was carried out by EDAX detector and EDX (Energy Dispersive X-Ray Analyzer). All these analyses were carried out on Quanta 450 Field Emission Gun (FEG).

3. Results and discussion

Tagetes erecta flowers extract was treated with silver nitrate to form the AgNPs by the reduction of Ag^+ into Ag^0. The colour change from light yellow to the dark brown of the reaction mixture displayed the formation of AgNPs (Fig. 1).

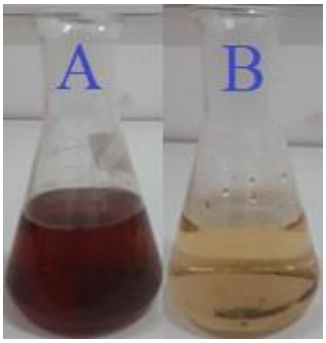

Fig. 1. Visual observation of biosynthesized AgNPs (A) vs. Tagetes erecta flowers extract (B) (color online)

As mentioned, the reduction of Ag^+ to Ag^0 was firstly confirmed by the colour change of the reaction mixture from light yellow to dark brown. In addition, monitoring the reaction progress by UV-Vis absorption spectroscopy supported the formation of AgNPs (Fig. 2). The UV-Vis spectrum of *Tagetes erecta* mediated synthesis of AgNPs have a strong band in the visible region (350-550 nm), with a maximum absorption peak (SPR band) at 422 nm. Furthermore, the presence of a single SPR band in the UV-Vis spectrum in the region of 410-500 nm supported the formation of spherical AgNPs [28, 29].

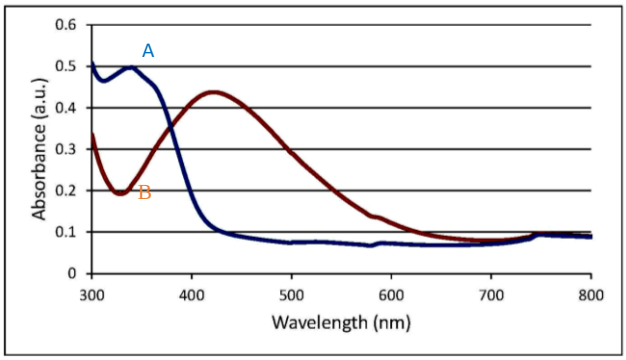

Fig. 2. UV-Vis absorption spectra of Tagetes erecta extract (A) and AgNPs (B) (color online)

FTIR analysis (Fig. 3) was performed for extract and AgNPs to elucidate the plausible natural products responsible for surface coating and efficient stabilization of AgNPs. The slight differences between the extract and AgNPs could be due to the oxidation of some molecules in extract by the reduction of silver ions. Table 1 shows the FTIR band assignment for "green" synthesized AgNPs. The functional groups displayed in Table 1 belong to biomolecules (polyphenols, proteins, ethers, and esters) arising from *T. erecta* extract, which are responsible for silver ions reduction and for AgNPs capping.

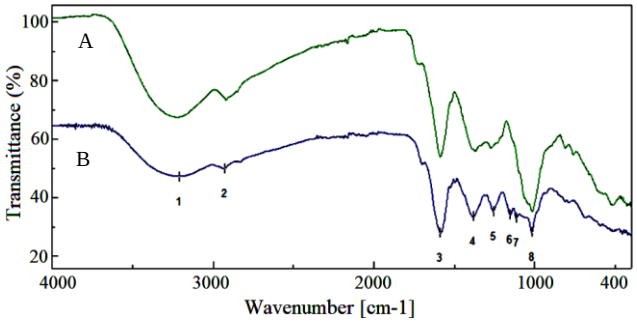

Fig. 3. IR spectrum of extract (A) and AgNPs (B) (color online)

Table 1. FTIR bands assignment of AgNPs synthesized from T. erecta flowers

FTIR Bands (cm^{-1})	Attribution	Ref.
3212	OH bending and stretching vibrations in the phenolic compounds.	[30]
2928	Asymmetric stretching of C-H bonds.	[31]
1587	Amine, NH bending	[32]
1383	Phenol, OH bending	[33]
1257	Aromatic ester, CO stretching, alkyl aryl ether, CO stretching	[34]

The crystalline nature of AgNPs was evaluated by X-ray diffraction analysis (Fig. 4). XRD patterns at 38.1°, 44.3°, 64.4° and 77.4° corresponding to the Miller indices of the reflecting planes (111), (200), (220) and (311), respectively, could be indexed to the face-centred cubic (fcc) crystalline structure of silver (JCPDS No. 87-0720) [35]. The size of silver nanoparticles was calculated by the Debye-Scherrer formula:

$$D = 0.9\,\lambda / \beta \cos\theta \qquad (1)$$

in which D is the average crystalline size (nm), λ is the X-ray wavelength (nm), β is the full width at half maximum intensity (FWHM) of the diffraction peak of the sample (radian) and θ is the Braggs angle (deg). The average size of AgNPs was calculated as 80.10 nm.

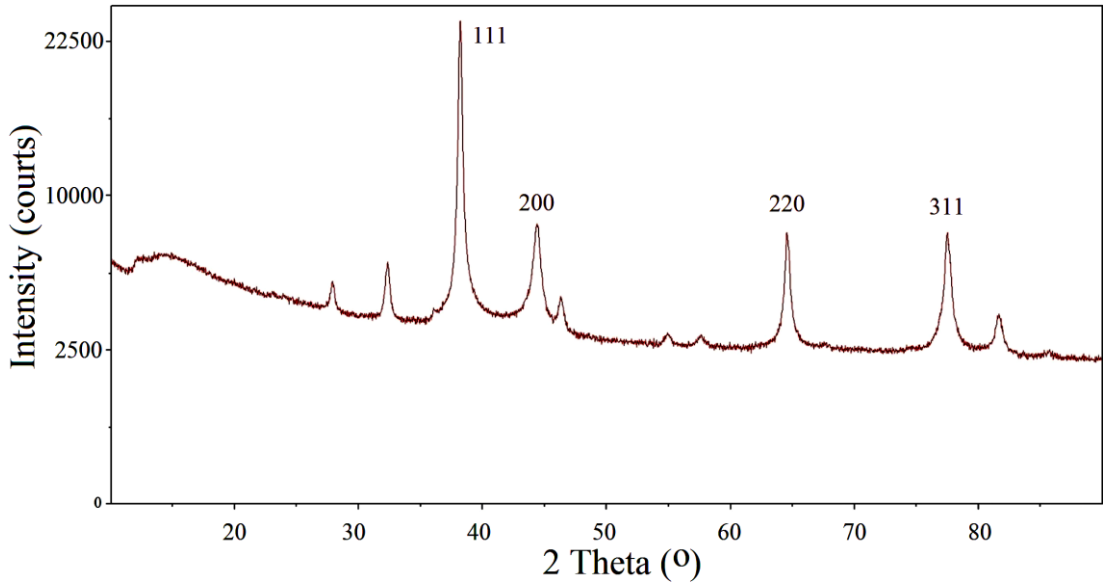

Fig. 4. XRD pattern of the obtained AgNPs in this study (color online)

Furthermore, the morphology of obtained AgNPs was studied by SEM image (Fig. 5) also presented the dispersion of agglomerated clusters which were distributed with a large random of empty space.

The energy-dispersive X-rays analysis of (EDX) supported the AgNPs formation. In addition, intense peaks in EDX spectrum at around 3 and 3.5 keV proved the presence of AgNPs structure. The carbon and gold peaks

appearing in EDX spectrum were due to the experimental condition (Fig. 5).

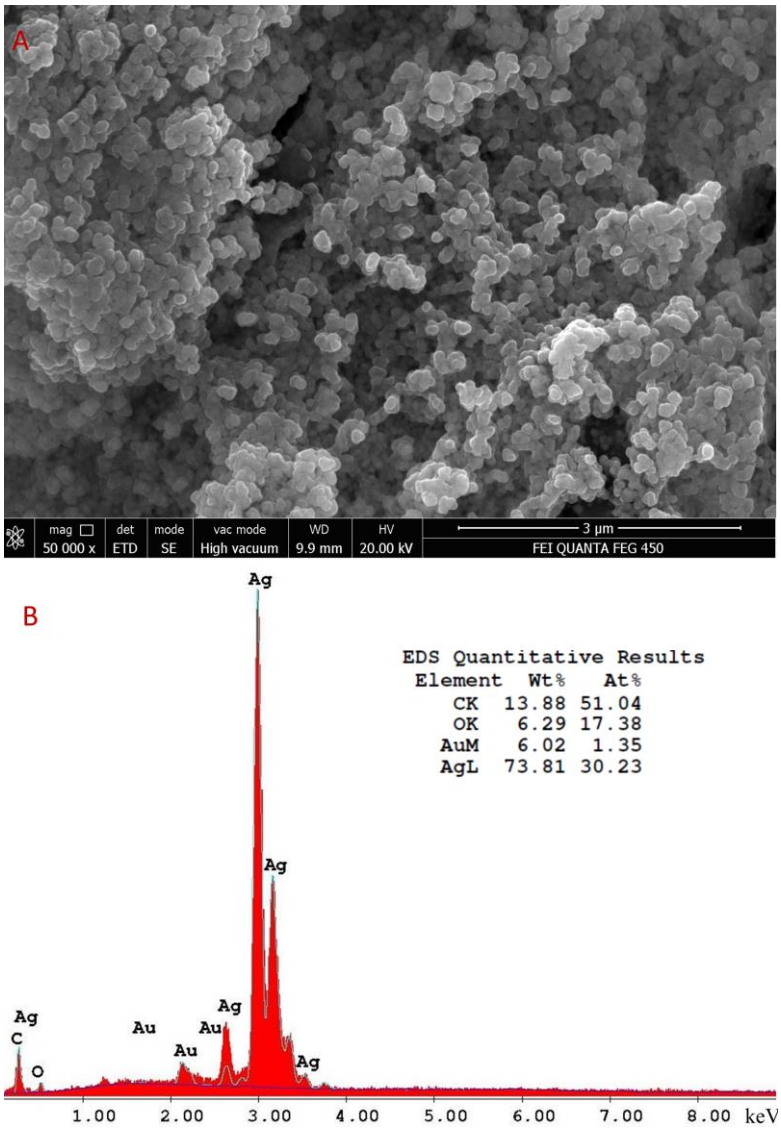

Fig. 5. SEM image (A), and EDX spectrum (B) of AgNPs (color online)

4. Conclusion

Efficient, low-cost, precise, eco-friendly biosynthesis of silver nanoparticles was achieved using an aqueous extract of *Tagetes erecta* L. flowers. This vegetal extract proved to be a good material for the biosynthesis of AgNPs with a fast and convenient method. The biosynthesis of AgNPs using *Tagetes erecta* flowers provided an important point of view to the nanotechnology for medicine, this plant being used efficiently in traditional medicine, due to the content of bioactive compounds in its flowers. AgNPs synthesized from this plant can be useful in biomedical applications as well as in the field of further research in nanobiotechnology.

References

[1] P. Koysu, N. Genc, M. Elmastas, H. Aksit, R. Erenler, Nat. Prod. Res. **33** (24), 3592 (2019).
[2] N. Genç, İ. Yıldız, T. Karan, Ö. Eminağaoğlu, R. Erenler, Turk J. Biodiv. **2**(1), 1 (2019).
[3] E. Dede, N. Genc, M. Elmastas, H. Aksit, R. Erenler, Nat. Prod. J. **9**(3), 238 (2019).
[4] T. Karan, I. Yildiz, A. Aydin, R. Erenler, Rec. Nat. Prod. **12**(3), 273 (2018).
[5] T. Karan, S. Simsek, I. Yildiz, R. Erenler, Int. J. Sec. Metabol. **5**(2), 87 (2018).
[6] R. Erenler, İ. Telci, M. Elmastaş, H. Akşit, F. Gül, A. R. Tüfekçi, İ. Demirtaş, Ö. Kayir, Turk J Chem **42**(6), 1695 (2018).
[7] M. Rafique, I. Sadaf, M. S. Rafique, M. B. Tahir, Artif Cells Nanomed Biotechnol **45**(7), 1272 (2017).

[8] M. E. Barbinta-Patrascu, C. Ungureanu, D. Besliu, A. Lazea-Stoyanova, L. Iosif, Optoelectron. Adv. Mat. **14**(9-10), 459 (2020).
[9] M. E. Barbinta-Patrascu, J. Optoelectron. Adv. M. **22**(9-10), 523 (2020).
[10] M. E. Barbinta-Patrascu, N. Badea, C. Ungureanu, D. Besliu, S. Antohe, Rom. Rep. Phys. **72**(3), 606 (2020).
[11] S. Jadoun, R. Arif, N.K. Jangid, R. K. Meena, Environmental Chemistry Letters **19** (1), 355 (2021).
[12] R. Arif, R. Uddin, Medical Devices & Sensors **4**(1), e10158 (2021).
[13] P. S. Nayab, R. Arif, M. Abid. In Recent Trends in Nanomaterials; Springer, 49 (2017).
[14] A. A. Kajani, A.-K. Bordbar, S. H .Z. Esfahani, A. R. Khosropour, A. Razmjou, RSC Adv. **4**(106), 61394 (2014).
[15] S. Bhakya, S. Muthukrishnan, M. Sukumaran, M. Grijalva, L. Cumbal, J. F. Benjamin, T. S. Kumar, M. Rao, RSC Adv. **6**(84), 81436 (2016).
[16] E. Burlacu, C. Tanase, N.-A. Coman, L. Berta, Molecules **24**(23), 4354 (2019).
[17] T. A. J. de Souza, L. R. R. Souza, L. P. Franchi, Ecotox Environ Safe **171**, 691 (2019).
[18] K. B. Narayanan, N. Sakthivel, Advances in colloid and interface science **156**(1-2), 1 (2010).
[19] A. Rana, K. Yadav, S. Jagadevan, Journal of Cleaner Production, 122880 (2020).
[20] J. R. Peralta-Videa, Y. Huang, J. G. Parsons, L. Zhao, L. Lopez-Moreno, J. A. Hernandez-Viezcas, J. L. Gardea-Torresdey, Nanotechnol. Environ. Eng. **1**(1), 1 (2016).
[21] M. Jiang, Y. Xu, L. Wang, J. Liu, J. Yu, H. Chen, Mitochondrial DNA Part B **5**(3), 2966 (2020).
[22] A. A. Safar, A. O. Ghafoor, D. Dastan, Pol. J. Environ. Stud. **29**(3), 2317 (2020).
[23] M. Hojnik, M. Škerget, Ž. Knez, LWT-Food Science and Technology **41**(10), 2008 (2008).
[24] W. Gau, H.-J. Ploschke, C. Wünsche, J. Chromatogr. A **262**, 277 (1983).
[25] B. Chitrakar, M. Zhang, B. Bhandari, Trends Food Sci. Technol. **89**, 76 (2019).
[26] H. Padalia, P. Moteriya, S. Chanda, Arab. J. Chem. **8**(5), 732 (2015).
[27] M. Zahran, M. El-Kemary, S. Khalifa, H. El-Seedi, Green Process Synth. **7**(2), 100 (2018).
[28] M. Rai, A. Yadav, A. Gade, Biotechnol Adv **27**(1), 76 (2009).
[29] Z. Zaheer, Colloids Surf B Biointerfaces **90**, 48 (2012).
[30] I. Zgura, M. Enculescu, C. Istrate, R. Negrea, M. Bacalum, L. Nedelcu, M. E. Barbinta-Patrascu, Nanomaterials **10**(11), 2146 (2020).
[31] S. N. Kharat, V. D. Mendhulkar, Mater Sci Eng C **62**, 719 (2016).
[32] M. Bindhu, M. Umadevi, Spectrochim. Acta A Mol. Biomol. Spectrosc. **128**, 37 (2014).
[33] S. Lokina, A. Stephen, V. Kaviyarasan, C. Arulvasu, V. Narayanan, Eur. J. Med. Chem. **76**, 256 (2014).
[34] G. Suresh, P. H. Gunasekar, D. Kokila, D. Prabhu, D. Dinesh, N. Ravichandran, B. Ramesh, A. Koodalingam, G. V. Siva, Spectrochim. Acta A Mol. Biomol. Spectrosc. **127**, 61 (2014).
[35] S. B. Aziz, G. Hussein, M. Brza, S. J. Mohammed, R. T. Abdulwahid, S. Raza Saeed, A. Hassanzadeh, Nanomaterials **9**(11), 1 (2019).

*Corresponding author: rerenler@gmail.com